Tectonics

RESEARCH ARTICLE
10.1029/2018TC005041

Key Points:
- Zircon He ages influenced by accumulated radioactive damage of crystals were partially reset by Cretaceous Paraná LIP
- Apatite He ages were completely reset and record a cooling event between 75 and 55 Ma by erosion of an up to 2-km thick cover layer
- Raman spectroscopy-based zircon radiation damage ages are comparable to He ages

Supporting Information:
- Supporting Information S1
- Table S1

Correspondence to:
M. Hueck,
mathiashueck@gmail.com

Citation:
Hueck, M., Dunkl, I., Heller, B., Stipp Basei, M. A., & Siegesmund, S. (2018). (U-Th)/He Thermochronology and zircon radiation damage in the South American passive margin: Thermal overprint of the Paraná LIP? *Tectonics*, *37*, 4068–4085. https://doi.org/10.1029/2018TC005041

Received 28 FEB 2018
Accepted 28 SEP 2018
Accepted article online 4 OCT 2018
Published online 29 OCT 2018

(U-Th)/He Thermochronology and Zircon Radiation Damage in the South American Passive Margin: Thermal Overprint of the Paraná LIP?

Mathias Hueck[1], István Dunkl[1], Beatrix Heller[1], Miguel Angelo Stipp Basei[2], and Siegfried Siegesmund[1]

[1]Geoscience Centre, Goettingen University, Göttingen, Germany, [2]Instituto de Geociências, Universidade de São Paulo, São Paulo, Brazil

Abstract New zircon and apatite (U-Th)/He data (AHe and ZHe) from the crystalline basement of the South American passive margin in southern Brazil present a wide distribution of Phanerozoic apparent ages, recording its prerift evolution. Its geological significance can be investigated by modeling the influence of the accumulated radiation damages on the measured crystals in its He ages during a long upper crust residence. Despite the presence of a significant fault in the studied area, the samples essentially constrain a uniform thermal history for the entire study area. Zircon helium ages spread from 472 to 26 Ma and correlate strongly with the radioactive element content of the crystals. Although the region was probably covered by Paleozoic sediments of the Paraná Basin, the ZHe system experienced a more intense thermal overprint, most likely the onset of the Paraná Large Igneous Province (LIP), causing its dispersion. The nearby intrusion of a feeding system of the LIP, the Florianópolis Dyke Swarm, may have contributed for keeping geothermal gradients elevated for a period long enough to promote the observed reset. After the extrusion of the volcanism, the study area was probably covered by up to 2 km of basalt floods, imprinting temperatures above the AHe partial retention zone on the crystalline basement. These were eroded during rapid cooling between 75 and 55 Ma, as indicated by thermal modeling. Additional analyses with Raman spectroscopy were used for calculating radiation damage ages in the zircon crystals measured for (U-Th)/He, resulting in a comparable set of ages.

1. Introduction

The Atlantic coast of South America is a classic area in the study of passive margin development. After the assembly of southwest Gondwana in the end of the Neoproterozoic, the area experienced Paleozoic intracratonic sedimentation and rift-related tectonics in the Cretaceous during the opening of the South Atlantic Ocean (Moulin et al., 2010; Zalán et al., 1990). This was immediately preceded by the onset of the Paraná Large Igneous Province (LIP) in the Lower Cretaceous, when volcanic floods with thickness of up to 2 km were extruded, mostly between 135 and 131 Ma, covering an area of more than 1,000 km^2 in South America and Africa (Janasi et al., 2011; Milani et al., 2007; Renne et al., 1992; Thiede & Vasconcelos, 2010). Intense exhumation followed the continental breakup, leading to the uplift of ridges in south and southeast Brazil with elevations of thousands of meters. Most thermochronologic studies have focused on these areas, recognizing the effect of rift and postrift exhumation (Cogné et al., 2011, 2012; Franco-Magalhães et al., 2010, 2014; Hackspacher et al., 2004, 2007; Hiruma et al., 2010; Jelinek et al., 2014; Ribeiro et al., 2005; Tello Saenz et al., 2003). The prerift evolution, however, is better detailed in areas with less dramatic topography, on which fission track and (U-Th)/He cooling ages commonly have disperse Paleozoic ages (Hueck et al., 2017; Kollenz et al., 2016; Oliveira et al., 2015).

(U-Th)/He thermochronology is one of the most used methods for investigating low-temperature thermal histories. An important development of the method in recent years is the understanding of the influence of a crystal's radioactive content in its He diffusivity, and how it can lead to varying closure temperatures within a same geological context (Flowers et al., 2009; Guenthner et al., 2013). This is particularly important in old stable areas with prolonged residence in near-surface conditions, on which the long accumulation of radiation damage amplifies this effect (Ault et al., 2009; Flowers & Kelley, 2011; Guenthner et al., 2017; Johnson et al., 2017; Murray et al., 2016; Orme et al., 2016; Powell et al., 2016). In these cases, it is possible to use the concentration of radioactive elements in each measured crystal, expressed in its effective uranium content (eU, U + 0.235 × Th, in ppm), as a tool for constraining detailed thermal histories.

In this paper we investigate the Phanerozoic history of a restricted segment of the South American passive margin using zircon and apatite (U-Th)/He thermochronology. Thermal and eU-based modeling is successfully applied to reconstruct the area's Phanerozoic history and investigate the thermal imprint of the Paraná LIP. The chosen study area comprises Neoproterozoic units of the Dom Feliciano Belt, and includes a prominent crustal discontinuity, the Major Gercino Shear Zone (Basei et al., 2000; Passarelli et al., 2010). One of the work's aims is to identify the impact this structure had in the low-temperature geochronological record (e.g., Ault et al., 2009; Cogné et al., 2011; Schultz et al., 2017; Sueoka et al., 2012; Tagami, 2012). Finally, we also explore the potential of applying zircon radiation damage assessment by Raman spectroscopy as a companion for the mineral's (U-Th)/He investigation.

2. Geological Setting

The Brazilian Platform is an assembly of cratons enveloped by Neoproterozoic orogenic belts that were juxtaposed in the Brasiliano (Pan-African) Orogenic Cycle (Almeida et al., 1981; Brito Neves & Fuck, 2014; Heilbron et al., 2008). The southernmost of these orogens is the Dom Feliciano Belt (DFB), stretching from Uruguay to south Brazil for over 1,100 km. It was formed by the tectonic interaction of the Río de la Plata, Congo, and Kalahari cratons, together with several microplates, juxtaposed along major shear zones (Basei et al., 2000; Hueck et al., 2018; Oriolo et al., 2016; Oyhantçabal et al., 2009; Philipp et al., 2016).

The northern portion of the DFB is exposed in a 60-km-wide corridor of basement rocks in the Brazilian state of Santa Catarina, called the Catarinense Shield. The belt is bordered to the north by the Luís Alves Microplate, which acted as the cratonic foreland during the Neoproterozoic (Basei et al., 2009; Passarelli et al., 2018). To the west and to the south, the crystalline basement is covered by the Paleozoic to Mesozoic sediments of the intracratonic Paraná Basin (e.g., Milani et al., 2007; Zalán et al., 1990), while to the east it is limited by the South Atlantic coastline. Throughout its extension, the DFB can be divided into three sectors (Basei et al., 2000). This is clearest in Santa Catarina, where each sector is separated from the next by major tectonic contacts.

The southeast domain corresponds to the Florianópolis Batholith, a multistage collection of plutonic suites associated to strongly reworked gneissic basement (Bitencourt & Nardi, 2000; Silva et al., 2002). The central domain consists mainly of the Brusque Group a metavolcano-sedimentary assemblage, and its crystalline basement, the Camboriú Complex (Basei, Campos Neto, et al., 2011, Basei et al., 2013; Philipp et al., 2004). Both units are intruded by voluminous granitic magmatism (e.g., Hueck et al., 2016). Finally, the northwest domain comprises the Foreland Itajaí Basin, an Ediacaran sedimentary package up to 5-km thick inverted by the end of the Brasiliano Cycle (Basei, Drukas, et al., 2011; Guadagnin et al., 2010).

Separating the southeast and central domain, the Major Gercino Shear Zone (MGSZ) is the main structural feature of the Catarinense Shield (Figure 1). It is characterized by kilometer-wide mylonite belts enveloping sin-transcurrent granitic intrusions (Bitencourt & Kruhl, 2000; Oriolo et al., 2018; Passarelli et al., 2010). Together with its extension in southernmost Brazil and Uruguay, the Dorsal do Canguçu, and Sierra Ballena Shear Zones, respectively, it forms a lineament over 1,000 km-long that has been interpreted as a former suture zone (Basei et al., 2000; Passarelli et al., 2011).

All three domains were juxtaposed in the Neoproterozoic during the assembly of the orogenic belt. Regional metamorphism was accompanied by reworking of the basement inliers in a converging setting between 650 and 620 Ma (Basei, Campos Neto, et al., 2011, Basei et al., 2013; Chemale et al., 2012; Hueck et al., 2018; Philipp et al., 2004). Most transcurrence within the MGSZ took place between 615 and 585 Ma, coupled to intense granitic magmatism in all domains that extended until ~570 Ma (Florisbal et al., 2012; Hueck et al., 2016; Passarelli et al., 2010). Deposition within the Itajaí Basin is constrained between 595 and 550 Ma (Basei, Drukas, et al., 2011; Guadagnin et al., 2010). Late-stage deformation is recorded in thrusting of the Brusque Group over the Itajaí Basin and reactivation of the shear zones until ~520 Ma (Passarelli et al., 2010; Rostirolla et al., 1992). At this point, the main geotectonic units in southwestern Gondwana had been juxtaposed, and exhumation is recorded in midrange geochronological data in Africa (e.g., Foster et al., 2009; Gray et al., 2006; Goscombe et al., 2005) and low-temperature thermochronology in the DFB (Hueck et al., 2017).

The Phanerozoic saw the development of the large intracratonic Paraná Basin. Two main supersequences were deposited in large internal seas with connection to the ocean during the Devonian and Permian, followed by two more deposition cycles in continental settings during the Mesozoic (Assine et al., 1994;

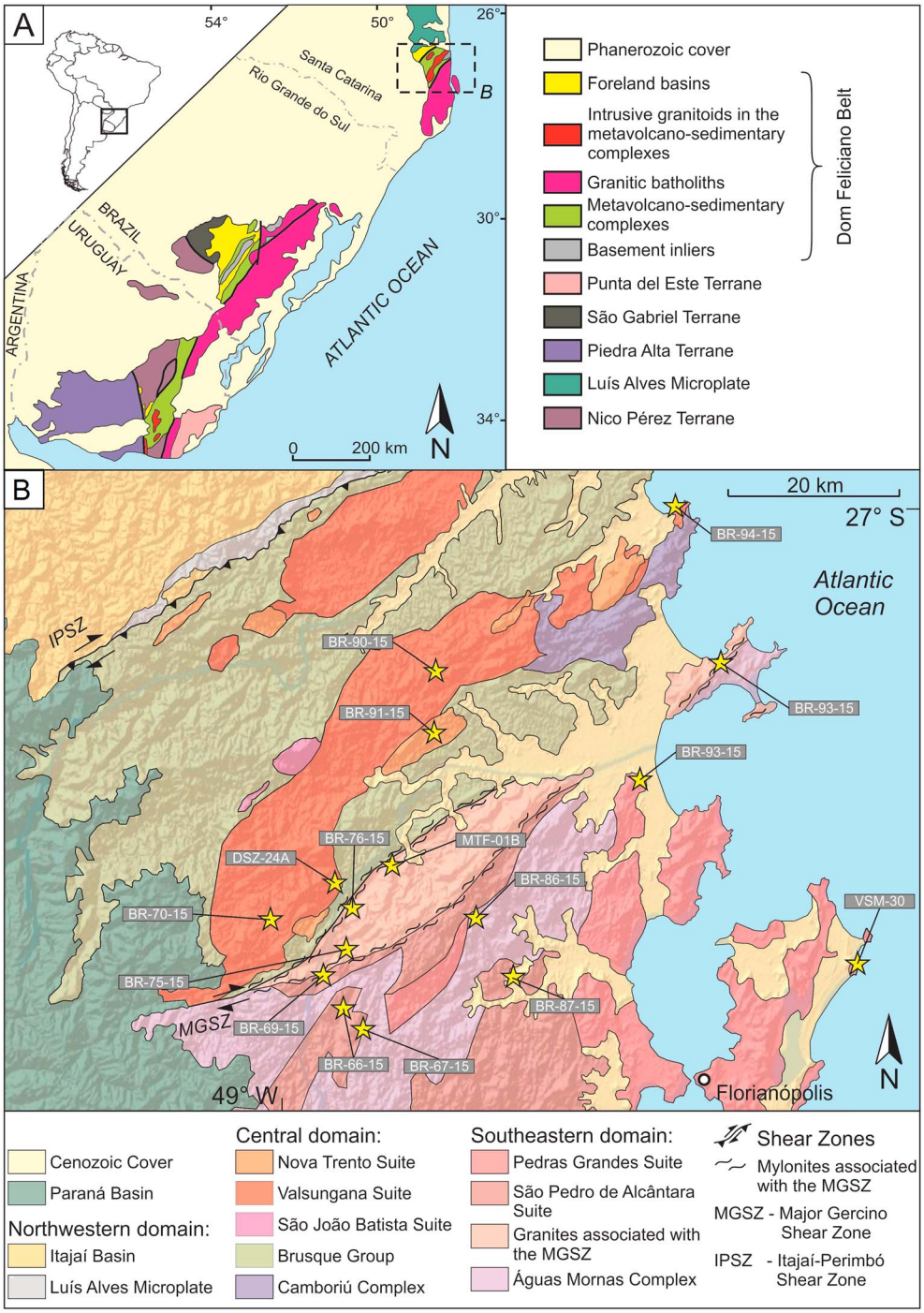

Figure 1. Geological map of the Major Gercino Shear Zone, with location of the analyzed samples (modified from Basei et al., 2000, 2006; Hueck et al., 2018; Passarelli et al., 2010).

Holz et al., 2010; Milani et al., 2007; Riccomini, 1997; Zerfass et al., 2004). The control of subsidence cycles and sedimentary gaps in the Paraná Basin is commonly linked to the far-flung influence of the Perigondgwanian orogenic processes in the southern border of the supercontinent (e.g., Rocha Campos et al., 2007; Zalán et al., 1990).

The geodynamic context of the Paraná Basin was spectacularly disrupted in the Early Cretaceous with the eruption of the massive continental flood basalts of the Paraná LIP. This event culminated in the extrusion

of volcanic rocks with a thickness of up to 2 km over an area of more than 1 $\times 10^6$ km^2 with remnants in Namibia and Angola. The majority of the lavas from this event were generated in a relatively short period, between 135 and 131 Ma (Ernesto et al., 1999; Janasi et al., 2011; Renne et al., 1992; Thiede & Vasconcelos, 2010). Vestiges of the feeding system of this event are preserved in Santa Catarina in the Florianópolis Dyke Swarm, comprising numerous doleritic dykes with a NNE-SSW direction (e.g., Florisbal et al., 2014). The extrusion of the continental basaltic magmatism in the Paraná Basin was followed by the initial opening and seafloor spreading of the South Atlantic Ocean from the Hauterivian to the Albian, as recorded in offshore basins of the South American Platform (Contreras et al., 2010; Moulin et al., 2010; Stica et al., 2014).

After the opening of the South Atlantic Ocean, the passive South American margin experienced intense exhumation, culminating in the uplift of coast-parallel ridges in south and southeast Brazil that frequently surpass 2,000 m in elevation. Those areas were traditionally the focus of most thermochronologic studies, and major exhumation cycles were recognized in the Upper Cretaceous-Paleocene and later in the Paleogene (Cogné et al., 2011, 2012; Hackspacher et al., 2004, 2007; Hiruma et al., 2010; Tello Saenz et al., 2003). Most studies correlate such cycles to episodes of alkaline magmatism and pronounced tectonic activity in the Andean system. This uplift, however, was not homogeneous along the coast. The area studied in this work presents a rather modest topography, mostly comprising elevations below 500 m. Recent research on such areas have revealed more detailed prerift exhumations stories (Hueck et al., 2017; Kollenz et al., 2016; Oliveira et al., 2015). The study area has not been the subject of detailed low-temperature research but is included by Karl et al. (2013) in a crustal block characterized by old zircon (U-Th)/He and fission track ages, limited by transverse SE-NW fault systems.

3. Samples and Methods

Samples were collected from the main basement units on both sides of the MGSZ along three cross sections (Figure 1 and coordinates in Table S1 in the supporting information). The majority of samples comprise the widespread granitic magmatism mainly intruded between 625 and 570 Ma. Over 30 samples were processed for zircon and apatite; after grinding and sieving, standard gravity and magnetic separation techniques were applied. According to the quality of the crystals, 16 samples were selected for thermochronologic analysis. All but two of them provided crystals from both mineral phases with the necessary quality for the (U-Th)/He analyses. The two remaining samples only had one of the minerals with a satisfactory quality. Three single-crystals aliquots were measured at the GÖochron Laboratory of the University of Göttingen for each sample, totalizing 45 He analyses each for zircon and apatite. In addition, Raman spectroscopy was applied to all measured zircon crystals prior to the He measurement, as a control of the radiation damage. Details of the laboratorial routine are described in Text S1 in the support information (Dunkl et al., 2008; Farley et al., 1996; Irmer, 1985; Lünsdorf & Lünsdorf, 2016). On many of the figures in this paper, results are divided into three groups in order to provide a better visualization. They correspond to samples collected in the central and southeast domain of the DFB and to samples from the MGSZ itself (Figure 1).

4. Results and Initial Observations

4.1. Zircon (U-Th)/He Data

The measured zircon (U-Th)/He (ZHe) ages are all younger than the emplacement/stratigraphic age of the sampled units. Single-crystal apparent ages show a large spread from 472 to 26 Ma (Table S2 in the support information). These ages do not correlate with elevation or grain size and are not dependent on location relative to the shear zone (Table S2 in the support information). However, there is a strong correlation between the ZHe ages and the eU content of corresponding crystals (Figure 2). Crystals with eU content below 1,000 ppm have a strongly negative correlation, while the youngest ages are restricted from 67 to 27 Ma, forming a long tail with eU contents between 1,000 and 5,200 ppm.

We assume that the wide spread of acquired ages is mainly controlled by their eU content. As such, the apparent ages probably do not represent geologically meaningful events, but rather variable eU-controlled closure temperatures within a partially reset ZHe system. The relative little intrasample variation, with most samples yielding multiple-crystal ages with in uncertainties between 6% and 20%, are the consequence of crystals from the same sample having similar eU contents.

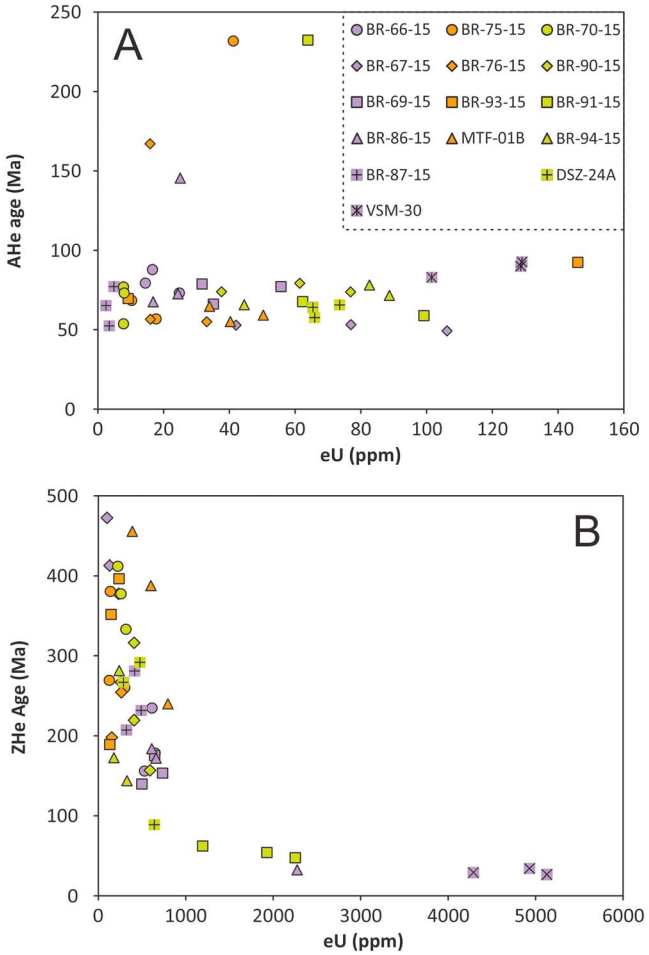

Figure 2. Single-crystal apatite (a) and zircon (b) (U-Th)/He age versus eU content for the entire data set. Different colors are used for different domains of the studied area in relation to the Major Gercino Shear Zone; purple, orange, and green symbols correspond to samples collected south of the shear zone, along its strike and north of it, respectively (as shown in Figure 1). Note that despite this distinction, all samples form a single coherent trend line.

The oldest ZHe age indicates that this thermochronometer has been partially closed since at least 472 Ma (Ordovician) in the study area. The combined results of crystals from all samples form a uniform coherent trend and can thus be assumed to record the same thermal history, representative for the entire study area. These assumptions will be used at the modeling of data, and an important approach will be to try to replicate the age distribution in relation to their eU content as predicted by the zircon radiation damage accumulation and annealing model (ZRDAAM, Guenthner et al., 2013).

4.2. Zircon Radiation Damage

The retentivity of He in zircon crystals is influenced by the damage inflicted in its crystalline lattice due to self-irradiation, which ultimately has an impact in the closure temperature of the ZHe method. Therefore, it is useful to develop companion techniques to examine the quality of a crystals internal structure prior to the (U-Th)/He analysis. Raman spectroscopy offers such an opportunity, using the width of the v3 (SiO_4) Raman band at ~1,000 cm^{-1} as a proxy for estimating the alpha-radiation damage (Nasdala et al., 2001; Palenik et al., 2003). Crystals with elevated damage will have broader peaks, which are expressed by the full width at half maximum (FWHM). The analyzed crystals have FWHM values that range from 2.3 to 21.7 cm^{-1}, but most crystals typically have values below 13 cm^{-1} (Table S2 of the support information).

Special care has to be taken when comparing results from the Raman and (U-Th)/He analyses, as there is a significant difference in the spatial resolution of these methods. While He ages and element concentrations are obtained from entire crystals, the Raman spots have diameters of only a few micrometers and depths of up to 20 μm and may therefore not be representative of the crystal as a whole. Nonetheless, despite of these issues, there is a moderate correlation between the FWHM values and the eU content of individual zircon crystals in our data set (Figure 3a). This is an indication that the Raman analyses are overall descriptive of the measured crystals, as the amount of alpha-radiation damage a zircon crystal has experienced is an expression of accumulation time and the content of U and Th. As eU and ZHe are strongly correlated in our data set, there is also a moderate negative correlation between FWHM and individual ZHe ages (Figure 3b).

In order to further explore these relationships, Figure 4 shows the correlation between FWHM values and eU content for each crystal, together with modeled radiaton damage isochrones spaced regularly at 100 Myr steps from 600 to 100 Ma. These isochrones were obtained using the empirical calibration curve of Palenik et al. (2003) and alpha-radiation damages calculated for each accumulation period and a range of eU concentations. Almost all measured zircons have FWHM values that correspond to the effect of the accumulation of 100 to 600 Ma of alpha-radiation damage.

Following this reasoning, zircon radiation damage ages can be calculated from the FWHM and U and Th concentrations (e.g., Pidgeon, 2014). The calculated ages vary from 61 to 957 Ma, but except for 5 of the 45 measured crystals, all values are younger than 510 Ma (Table S2 in the support information). The outlying ages are unrealistic, as they are older than the crystallization age of the sampled rocks.

To first order, the calculated ages correspond to the possible range of ages on which the zircons could have started accumulating radiation damage (Figure 5). Furthermore, they lie within an age interval that is very similar to the one obtained by the ZHe ages. It should also be noted that a clear majority of ages calculated from the radiation damage are older than the corresponding (U-Th)/He ages, evidencing a systematic difference between the thermal sensitivity of these systems. Additionally, there is a correlation between the

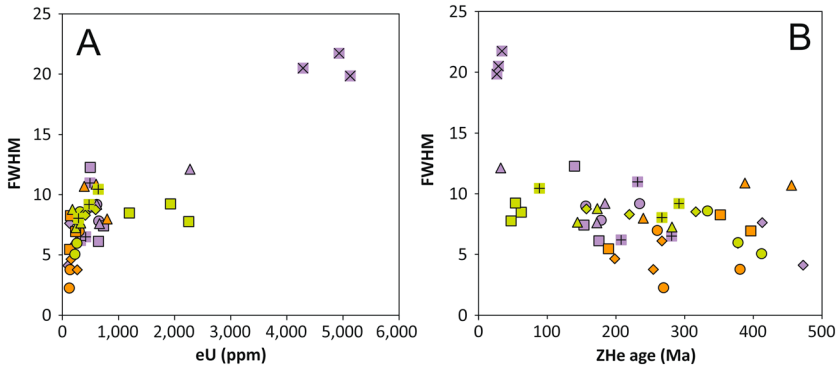

Figure 3. Full width at half maximum (FWHM) of the ~1,000 band in zircon vs. (a) single-crystal eU value and (b) single crystal ZHe age. Symbols used are the same as in Figure 2.

radiation damage ages and the corresponding crystal's eU values, with crystals with more elevated actinide contents generally yielding the youngest ages.

4.3. Apatite (U-Th)/He Data

Apatite (U-Th)/He (AHe) ages have a much smaller dispersion than the ZHe results. With the exception of a few outliers, single-crystal ages are tightly constrained between 93 and 49 Ma (Table S2 in the support information). Single crystals ages have little intrasample variation. Mean ages range from 89 to 52 Ma, and most uncertainties (2 SE) are within 6%, with only four samples surpassing 10%. The well-restrained data set indicates that all samples experienced a similar thermal history within the AHe thermal range, which can be considered as representative of the studied area.

There is no apparent correlation between AHe ages and other possible criteria, such as altitude, geographic position, crystal size, or eU content (Table S2 in the support information). Nonetheless, the data set includes crystals with a wide range of sizes (equivalent sphere radius between 31 and 94 μm) and eU contents (ranging from 2 to 146 ppm). Crystals with outlying AHe ages are well within the range of all measured parameters (e.g., grain size and eU content) and probably represent small and unaccounted for inclusions. Therefore, these ages were considered unrealistic and were discarded for all subsequent evaluations. The relatively short range of apparent AHe ages, combined with a lack of correlation with crystal size or eU content, suggest that measured crystals have not experienced prolonged residence in the partial retention zone (PRZ) of the AHe thermochronometer. Had this been the case, the impact of these factors in the AHe system would be reflected in a larger spread of apparent ages. Instead, the data set suggests a relatively quick cooling to near-surface temperatures from conditions under which the AHe system was completely open (above 60–80 °C) between 90 and 50 Ma, as constrained by the single-crystal ages.

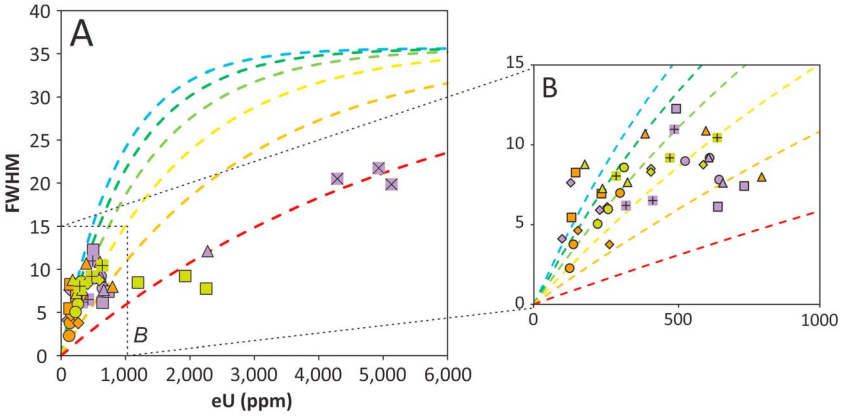

Figure 4. Full width at half maximum (FWHM) of the ~1000 cm^{-1} band in zircon versus single-crystal eU value and radiaton damage isochrones obtained using the empirical calibration curve of Palenik et al. (2003) spaced regularly at 100-Myr steps from 600 (blue) to 100 (red) Ma. Detail of (a) is presented in (b). Symbols used are the same as in Figure 2.

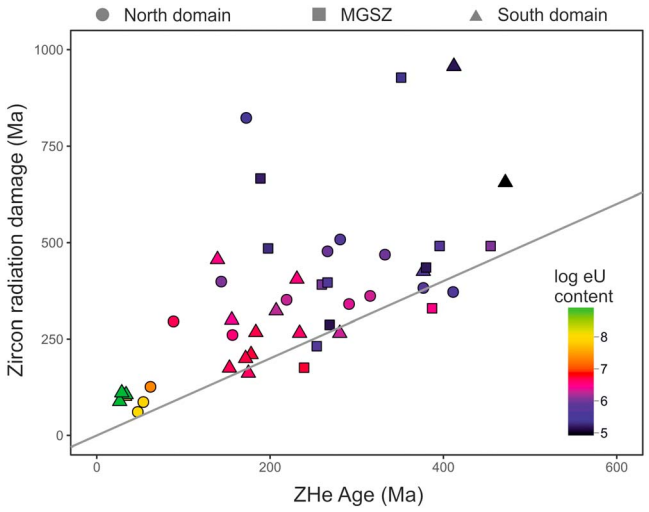

Figure 5. Single-crystal radiation damage ages versus measured zircon (U-Th)/He ages. Radiation damage ages were calculated after Pidgeon (2014) based on the measured peak width of the ~1,000 band in zircon and the empirical calibration curve from Palenik et al. (2003). In a simplified way, the ages correspond to the relative position of each crystal in relation to the radiation damage isochrones presented in Figure 3. Different symbols are used for different domains of the studied area in relation to the Major Gercino Shear Zone (MGSZ). The solid line represents a one-to-one correlation between the methods. Symbol colors correspond to the eU content of the analyzed crystals, as indicated by the legend.

5. Modeling the Thermal History

This section aims to investigate how the thermochronologic data set can be explained with geologically reasonable thermal trajectories. Any possible history has to be able to replicate both the spread of the ZHe data set and the relative constraint of the AHe results. For this, we applied a combination of eU-based and inverse thermal modeling with the HeFTy program (Ketcham, 2005) using the zircon ZRDAAM (Guenthner et al., 2013) and apatite RDAAM diffusion models (Flowers et al., 2009).

Modeling of the data set followed a two-step approach. The first step consisted of *eU modeling*, that is, using forward modeling for testing different thermal histories and comparing the calculated eU content versus ZHe age patterns to the measured data set (Guenthner et al., 2017; Johnson et al., 2017; Orme et al., 2016; Powell et al., 2016). Initially, a variety of possible thermal histories were tested in order to see what ZHe distributions would be generated. Subsequently, we tested variations of the most successful (and geologically most meaningful) *T-t* paths. This step was not applied to the apatite results, due to the relatively young apparent ages and the lack of age-eU correlation, which indicates a history of quick cooling between 90 and 50 Ma (e.g., Ault et al., 2009).

In the second step, inverse thermal modeling was used to evaluate how successfully the trajectories obtained in the eU models can be reproduced when testing both the ZHe and AHe results. For this, the simulations had a relative degree of freedom to explore for thermal paths, fixing only the necessary constraints in order to test a given scenario.

Four significant regional geological events were taken into account during modeling as constraint or as tested hypotheses. First, initial cooling from middle-temperature range (e.g., cooling temperatures of K-Ar system in muscovite) in the region happened between 600 and 500 Ma. Most dated samples are granites dated by U-Pb predominantly between 625 and 570 Ma (Basei, Campos Neto, et al., 2011; Chemale et al., 2012; Florisbal et al., 2012; Hueck et al., 2018; Passarelli et al., 2010), and mica K-Ar ages spread from 600 to 540 Ma (Passarelli et al., 2010). Second, deposition of Devonian and Permian sediments of the Paraná Basin may have covered the studied area. Based on the maturation of organic material, this burial did not impose temperature increases above 80–100 °C (Silva & Cornford, 1985). Third, we acknowledged the extrusion of the Paraná LIP, mostly constrained between 135 and 131 Ma (Janasi et al., 2011; Renne et al., 1992; Thiede & Vasconcelos, 2010). Heating associated to intrusion of feeding dykes and sills is interpreted as responsible for most of the overmatured organic material in the Paraná Basin (e.g., Zalán et al., 1990). Finally, surface temperatures for the present day were set at 20 ± 5 °C.

5.1. eU Modeling

In this step, forward modeling was used for testing different thermal histories with the zircon ZRDAAM diffusion model, in order to attempt to reproduce the range of measured apparent ZHe ages and its relation to the crystals' eU content. Input data used were the radius of a crystal's equivalent sphere, U and Th concentrations equivalent to a eU content spectrum between 100 to 5,000 ppm, and a given *T-t* path. For each tested scenario, we modeled three curves assuming three crystal sizes. The first one used a sphere radius corresponding to the mean value for all dated crystals (~50 μm), while the remaining comprise inner and outer envelopes by adding or subtracting two standard deviations to the mean (~20 μm). The resulting pattern was then compared to the entire ZHe data set.

On a first approach, the models aimed to test thermal trajectories corresponding to end-member crustal histories for the studied area, in order to see how the calculated eU curves react to paths controlled purely by each of the main geological event that affected the region (Figure 6a). First, we tested a simple exhumation to surface conditions shortly after cooling from midrange temperatures in the end of the Neoproterozoic. Second, sedimentary burial promoted by the Paraná Basin was simulated by adding to the first scenario a monotonic heating between 430 and 250 Ma up to 120 °C, corresponding to a conservative maximum

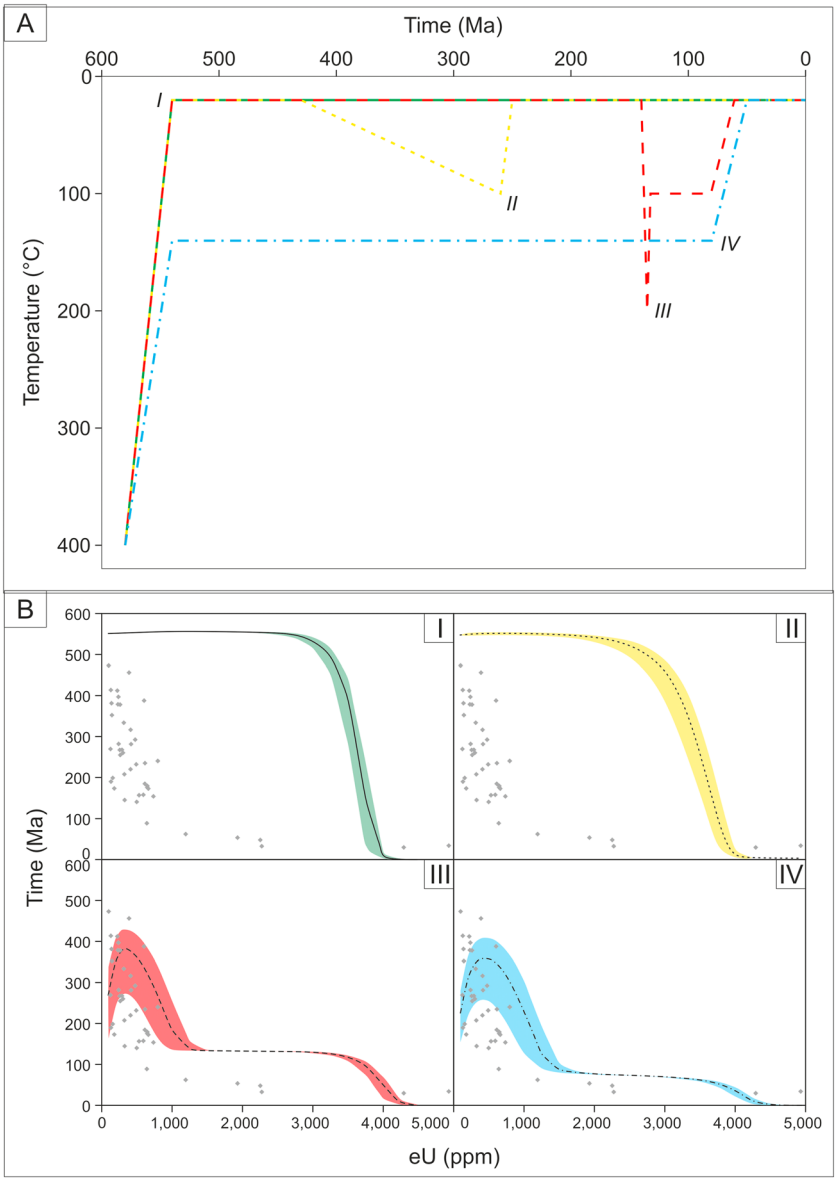

Figure 6. Diagram summarizing the results of thermal modeling considering all dated zircon crystal and calculated ZHe ages according to their eU content. (a) Tested end-member thermal scenarios. (b) Modeled zircon (U-Th)/He ages. Central lines were calculated for crystals with a corresponding sphere radius of 50 μm, while the envelope represents variations of 20 μm. The colors of the envelops correspond to the colors of the assumed thermal paths on (a).

thermal imprint of the Paleozoic sediments from the Paraná Basin (Silva & Cornford, 1985). On a third hypothesis, the onset of the Paraná LIP was simulated by fixing a heating event with maximum temperatures of 200 °C and total duration of 10 Myr starting from surface conditions at 140 Ma. This simulation considers that most of the LIP was extruded between 135 and 130 Ma (Janasi et al., 2011; Renne et al., 1992; Thiede & Vasconcelos, 2010) and assumes maximum temperatures that could result in a partial reset of the ZHe system, as is suggested by our data. This hypothesis also assumes that the extrusion of the LIP resulted in the addition of up to 2 km of volcanic rocks in the area, simulated by setting the temperature after the onset of the LIP at 100 °C and adding a last stage of exhumation between 90 and 50 Ma as constrained by the AHe data. Finally, a history of prolonged residence in the ZHe PRZ was modeled by fixing an initial cooling in the end of the Neoproterozoic to 140 °C and keeping this temperature until 80 Ma, after which we imposed a cooling to surface conditions by 50 Ma. This last cooling step is well constrained by the apparent AHe ages.

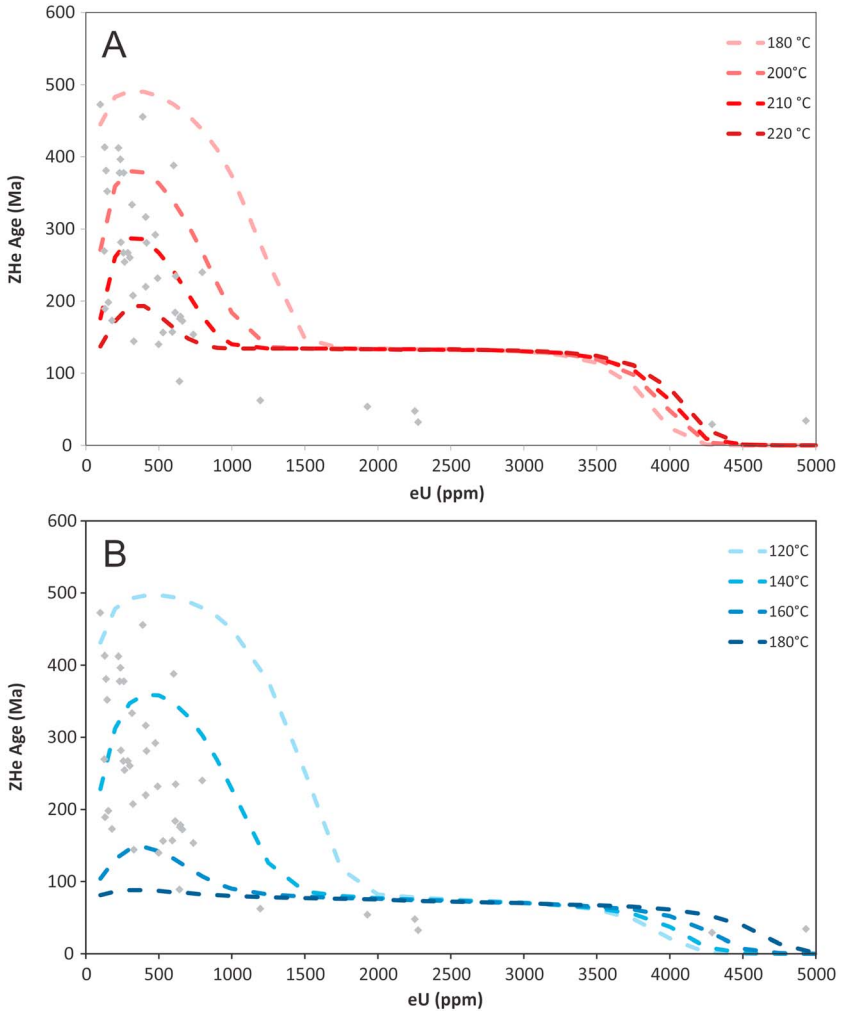

Figure 7. Sensitivity tests for scenarios III and IV of Figure 6. (a) Effect on the ZHe ages versus eU content distribution patterns of the variation of the maximum temperature of the short Cretaceous thermal pulse simulated in scenario III. For the sake of clarity, the final phase of exhumation in the Cretaceous simulated in Figure 6 is not included in this simulation. Tested temperatures range from 180 to 220 °C. (b) Effect on the ZHe ages versus eU content distribution patterns of the variation of the temperature of the prolonged exposure to Partial Retention Zone conditions simulated in scenario IV. Tested temperatures range from 120 to 180 °C. All curves were calculated for crystals with sphere radius of 50 μm.

The first two scenarios yield eU distributions evidently incompatible with the tested data set (Figure 6b). Exhumation to surface condition in the early Cambrian would generate uniformly old ages throughout most of the tested eU spectrum and would need a later thermal overprint in order to generate the spread in ZHe ages measured. In the next scenario tested, it is clear that this partial reset cannot be reached alone by the effect of the Paleozoic sedimentation of the Paraná Basin, since its maximum overprint only slightly resets crystals with relatively high eU contents (2,000 to 3,500 ppm).

On the other hand, the remaining hypotheses yield curves that are much closer to the general trend of the ZHe data set (Figure 6b). Both a rapid thermal imprint of the Paraná LIP in the Cretaceous and a prolonged period in the system's PRZ during the Paleo to Mesozoic are successful in generating apparent age patterns that are similar to the measured data set. In particular, they are characterized by markedly old ages within the eU range of 100 to 1,000 ppm, which is one of the main characteristics of the measured results.

In order to explore how well these two thermal histories replicate the measured ZHe data set, both scenarios were submitted to a sensitivity test. This consisted of varying the fixed temperatures assumed for simulating the geological events tested in the end-member scenarios (Figure 7). In the first case, four different maximum temperatures ranging between 180 and 220 °C were tested for the short Cretaceous thermal pulse, while in

the second case the long Paleo-Mesozoic residence in the PRZ was simulated with four different temperatures between 120 and 180 °C. The resulting patterns envelop almost the entirety of measured data. In other words, the range of apparent ages in the new data can mostly be reproduced only by adding or subtracting 20 °C from the central temperatures tested in the end-member scenarios. It should be noted that in order to keep the diagrams clear, Figure 6 only displays the curves for crystals with equivalent sphere radii corresponding to the mean measured value (50 μm). The same models with the entire range of measured radii would lead to an envelopment of the measured data with even smaller variations in the experienced temperature.

Despite the good agreement between the most successful models and the measured data set, none of the tested scenarios was able to capture the trend of crystals with eU contents >1,000 ppm. The measured ages of crystals with eU contents between 1,000 and 4,000 ppm are younger than those predicted by the models and are in fact comparable to those obtained for the AHe system. Considering the maximum possible time of damage accumulation for the sampled rocks, our models would only predict such comparable ages for crystals with eU contents, between 3,000 and 3,500 ppm. The inverse effect happens for crystals with eU contents >4,000 ppm, for which the modeled ages tend to zero, which is in disagreement with measured ages of a few tens of million years.

5.2. Thermal Modeling

The next step in modeling the data set consisted of inverse thermal modeling. In it, random *T-t* paths were tested and the resulting crystal diffusion curves were compared with the ones calculated from the input data. Satisfactory results were then categorized as acceptable or good paths (see Ketcham, 2005, for more details). In this way we tested that the most successful scenarios constrained in the first step (i.e., short Cretaceous thermal pulse and long Paleo-Mesozoic residence in the PRZ) are reproduced by the measured data set including both zircon and apatite results.

The tested models were designed with a certain degree of freedom, so as not to force the simulations to follow a tight *T-t* path. An initial constraint was set for both models corresponding to the age of cooling from midrange temperatures around 540–500 Ma (Passarelli et al., 2010). For the scenario of a partial reset caused by the thermal overprint of the Paraná LIP magmatism (scenario III in Figure 5b), exhumation to near-surface conditions (0–60 °C) was constrained for the early Paleozoic, before the onset of sedimentation in the Paraná Basin. Temperatures were then limited below 120 °C for much of the Paleo and Mesozoic, corresponding to the maximum possible heating promoted by the Paleozoic Sequences. Higher temperatures (up to 220 °C) were only allowed around the age of the magmatic event, between 140 and 130 Ma, after which the thermal range was again limited to below 120 °C. In the second scenario tested, considering a long residence in the ZHe PRZ (scenario IV in Figure 5b), the only constrain set was that the tested paths were not allowed to achieve temperatures below 60 °C until ~80 Ma.

Each simulation tested 100,000 different trajectories, or was interrupted after achieving 100 good paths. Three representative samples were tested for this simulation, one for each of the main tectonic units in the study area (southeast domain, along the MGSZ, and central domain). Each model considered the results of two crystals from each mineral phase. In addition, we tested a synthetic simulation combining the data set for the entire study area. The advantage of using such an approach is that it can be used to test different portions of the eU content spectrum obtained for each mineral, thus constraining thermal trajectories that better represent the complexity of the data set (e.g., Ault et al., 2009; Johnson et al., 2017). In our model, we separated the ZHe data by eU content into two bins that correspond to most of the measured crystals (less than 350 ppm and between 350 and 700 ppm), generating two synthetic crystal populations of which we used the average values of U and Th concentrations, and the mean radius of the equivalent sphere. Similarly, mean apatite results were selected for two eU ranges, of less than 20 ppm and between 60 and 100 ppm.

The tested models performed very well with the described inputs, generating numerous acceptable and good paths. Most scenarios provided 100 good paths before testing 100,000 individual trajectories. In this regard, none of the tested hypothesis clearly outperformed the other, and both represent viable geological histories for the measured (U-Th)/He data set. Furthermore, the different samples tested all provided similar results (Figure 8). Models simulating a short Cretaceous thermal pulse associated to the Paraná LIP resulted in good paths that reach up to the imposed limit of 220 °C for this event. As expected, this scenario constrains a

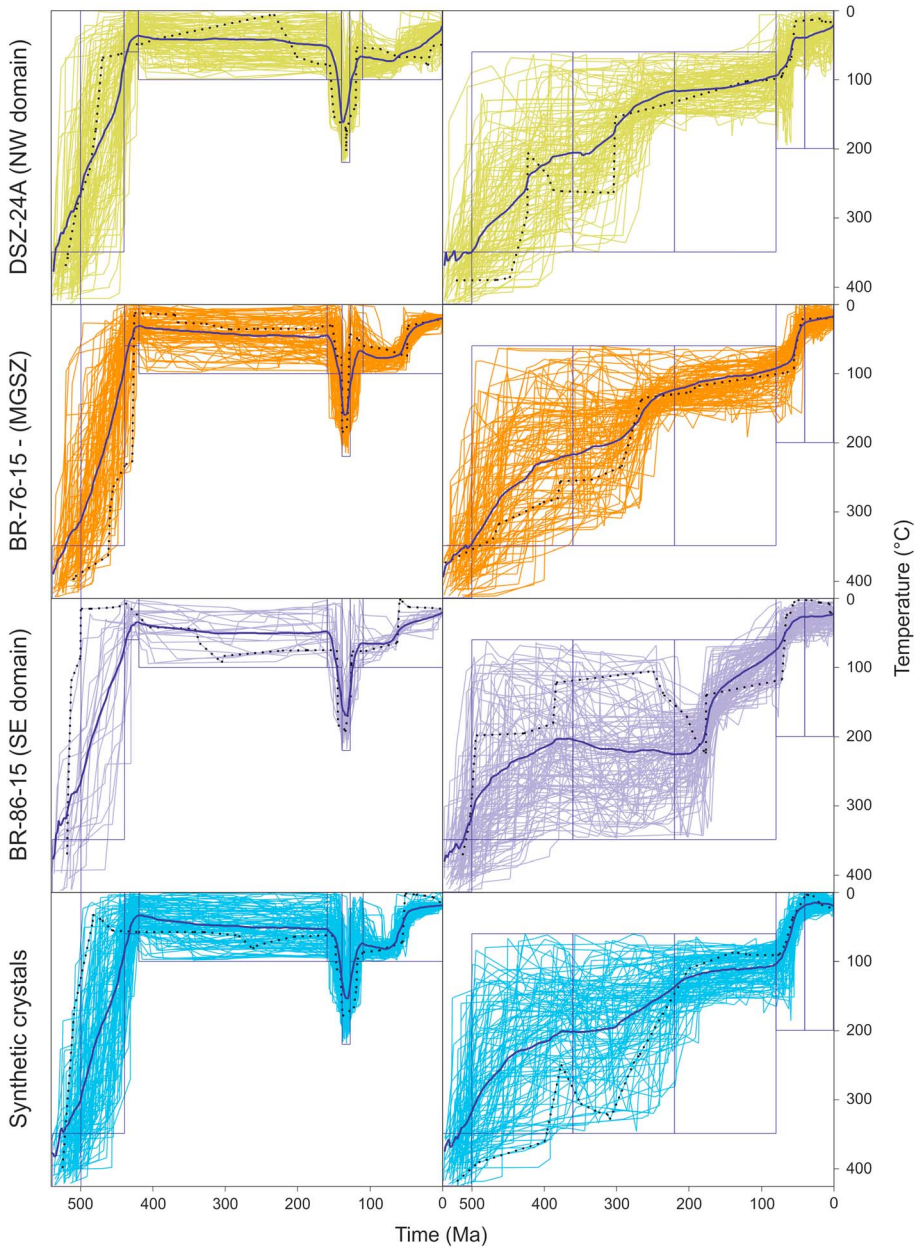

Figure 8. Thermal modeling results of the most likely histories, corresponding roughly to scenarios III and IV of Figure 6. Models were tested for three representative samples and for average values from a combination of synthetic crystal populations representative of the entire data set. Only paths classified as good fits by the program are displayed. Boxes represent the thermal constrained used in the simulations. MGSZ = Major Gercino Shear Zone.

last cooling event from ~60 to 110 °C to near-surface conditions between the end of the Cretaceous and the beginning of the Paleogene, corresponding to the complete reset of the AHe system. The models which simulated a prolonged residence in the PRZ yielded good paths that initially spread through the entire possible range of *T-t* trajectories before converging to temperatures between 80 and 160 °C in the Mesozoic. The most significant variation in the models is recorded in sample BR-86-15, from the southeast domain, in which a cooling event to temperatures below 180 °C was constrained at ~180 Ma, corresponding to the sample's apparent ZHe ages. The models using the averaged crystal populations as input have results that are entirely in accordance with those for the real samples and did not produce a more constrained thermal evolution.

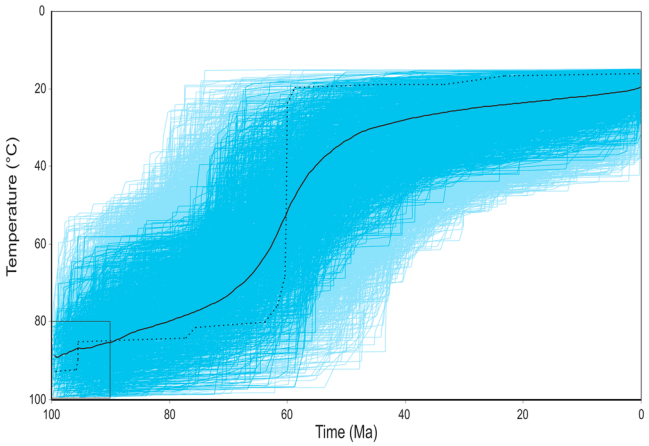

Figure 9. Unconstrained thermal modeling results of the AHe data set. Light and dark blue curves are paths classified as acceptable and good fits, respectively. Continuous line is the mean calculated trajectory and pointed line is the tested path with the best fit.

A last round of modeling tested only the AHe data set, aiming to explore the system's full eU range. For this step, the input considered the mean values for four crystal populations with ranges of <20, 20–60, 60–100, and > 100 ppm. In this simulation, the only constrain was a fixed starting point corresponding to temperatures and ages little above those constrained by the AHe data (90–100 Ma, 80–100 °C). This simulation then tested random *T-t* paths until achieving 1,000 good trajectories. The resulting good paths (Figure 9) define a more constrained age window for the cooling of the AHe system between 75 and 55 Ma, thus narrowing the broader time range obtained by the apparent ages (~50–90 Ma).

6. Discussion

6.1. Thermochronologic Control of the Zircon and Apatite He Ages

The eU-based models show that the significant spread of apparent ZHe ages observed in the study area is strongly controlled by the eU content of individual crystals. As such, instead of expressing geologically meaningful events, the apparent ages represent crystals with variable closure temperatures exposed to a same thermal history that cause partial reset of the ZHe system (e.g., Guenthner et al., 2015, 2017; Johnson et al., 2017; Orme et al., 2016; Powell et al., 2016). The eU content versus ZHe age pattern was successfully reproduced by testing geologically reasonable scenarios with the ZRDAAM model (Guenthner et al., 2013). These scenarios were, in turn, reproduced by inverse thermal modeling of the measured data set, further strengthening our interpretation. However, our models were not successful in predicting the ages of the more radioactive crystals. Crystals with eU content between 1,000 and 2,500 have ZHe ages similar to those of the AHe system and therefore probably represent similar closure temperatures. However, the ZRDAAM model only predicts such an effect for crystals with eU contents between 3,000 and 3,500 ppm. On the other hand, ZHe ages for crystals with eU > 4,000 ppm still retain enough He to yield ages of some tens of million years, although the predicted apparent ages should tend to zero, similar to that observed by Johnson et al. (2017). This could be the result of eU zonation causing *pockets* of He-retentive crystal lattices in overall highly radioactive zircon crystals (e.g., Danišík et al., 2017).

Together with the latest research focused on the potential of modeling the control of eU content on the ZHe system, the results presented here caution against the overinterpretation of apparent (U-Th)/He ages without a proper assessment of how He diffusivity has been affected by the crystals characteristics. This is particularly true to areas with ancient geological history, as the accumulation of radiation damage over time amplifies the influence of such features. Sampling strategies in such cases should therefore focus in measuring more crystals from a same sample, even at the expense of enlarging the possible study area. The acquisition of data sets with a wide range of crystal sizes and eU contents is particularly helpful.

The AHe data set, on the other hand, yielded results with the opposite behavior, producing ages that do not seem to be controlled by the expected crystal features, such as eU or crystal size (Flowers & Kelley, 2011; Guenthner et al., 2017; Murray et al., 2016). This indicates that the study area has probably not experienced a prolonged time in the system's PRZ (e.g., Ault et al., 2009). Thermal modeling was able to reproduce this interpretation, and define a cooling event between 75 and 55 Ma that would have caused a complete reset of the thermochronometer. The age spread surpassing this time period is probably caused by nonquantified crystal features such as internal zonation, implantation of He from radioactive neighboring minerals (so-called *bad neighbors*), Cl content and microinclusions (Ault & Flowers, 2012; Flowers & Kelley, 2011; Gautheron et al., 2013; Spiegel et al., 2009).

6.2. Phanerozoic Evolution of the Catarinense Shield

The measured (U-Th)/He data set is best explained by a shared geological history, as evidenced by the uniform coherent trends observed in the eU content versus ZHe/AHe age diagrams. Consequently, despite evidences of episodic Phanerozoic reactivation of shear zones in the Dom Feliciano Belt (Hueck et al., 2017; Oriolo et al., 2018), the MGSZ has not caused enough differential exhumation in order to leave a regional impact in the low-T thermochronometers.

The Ordovician apparent ZHe age of the oldest individual crystals implies that initial exhumation in the early Paleozoic exposed the crystalline basement, leading to the accumulation of both He and radiation damage in zircons since the early Paleozoic. This observation is in accordance with comparable ZFT and ZHe in the southern expositions of the Dom Feliciano Belt (Hueck et al., 2017; Oliveira et al., 2015) and implies in an early Paleozoic exhumation following the postcollisional stage of the belt. As pointed out by Hueck et al. (2017), this process possibly took place during the late stages of the Pan-African orogenic cycle in the Damara Orogen (Foster et al., 2009; Gray et al., 2006; Goscombe et al., 2005).

The wide dispersion of apparent ZHe ages indicates that this system was partially reset, with He diffusion being controlled by the crystals' radiation damage densities. By applying eU and inverse thermal modeling, two viable scenarios can satisfy this the regional geological context and the measured data set. The first one begins with exhumation to near-surface conditions before the sedimentation in the Paraná Basin, followed by a long period with temperatures below 120 °C, and only disrupted by the onset of the Paraná LIP around ~135 Ma. This event caused the partial reset recognized in the ZHe system and was later followed by a final stage of cooling between 75 and 55 Ma. Alternatively, the dispersion in the ZHe ages could be explained by a prolonged residency in the system's PRZ, particularly during most of the Mesozoic, later followed by an equivalent cooling event in the Late Cretaceous to early Paleogene.

Both hypotheses are possible considering the thermochronologic data set. However, a surface exposure of the crystalline basement during the Paleozoic is very likely, as the base of the Devonian sediments of the Paraná basin is situated less than 10 km to the west of the studied area, with no significant fault system known in between. Consequently, the study area has probably been exposed to near-surface conditions in the past and had to experience a later thermal overprint in order to justify its ZHe data. Although Paleozoic burial is certainly possible, and even likely given the reasons just discussed, our models show that this alone could not have promoted enough He loss so as to induce the dispersion in the zircon ages.

As a consequence, partial reset caused by the thermal imprint from the Paraná LIP seems to be the most likely cause of the ZHe scatter. This observation is somewhat surprising, as thermal simulations suggest that the flood basalts should not have left a significant thermal imprint in rocks not within close range, due to fast cooling within hundreds of thousand years (Hurter & Pollack, 1994). The identified thermal overprint, however, could be explained by the existence in the region of an important feeding dyke system of the Paraná LIP in the Catarinense Shield, the Florianópolis Dyke Swarm, (e.g., Florisbal et al., 2014). We propose that the continuous intrusion of basaltic dykes in the crystalline basement throughout the duration of the LIP could have provided the necessary thermal gradients in order to affect the ZHe system. It has been suggested that the coast-parallel orientation of dyke swarm, perpendicular to most of the dykes recognized in southern Brazil, might be an evidence of its proximity to the South Atlantic rift center or even to the head of the mega-plume suggested by some authors as responsible for the Paraná LIP (Salomon et al., 2017, and references therein). Such a position would further contribute to elevated geothermal gradients in the region.

The extrusion of the Paraná LIP probably left a cover of massive basaltic floods in the study area, such as those preserved in other parts of the basin. This is evidenced by the fact that the AHe system remained open after the magmatic event, only closing by the Late Cretaceous-early Paleogene, when the volcanic cover, probably associated with remaining sedimentary sequences of the Paraná Basin, were eroded. The existence of the Florianópolis Dyke Swarm has also been argued as evidence that the Catarinense Shield should have been covered by basaltic floods, connecting the remains of the Paraná LIP in South America to its counterparts in Africa (Florisbal et al., 2014). Thermal modeling considering the AHe data set constrain this exhumation event between 75 and 55 Ma, when most successful thermal simulations suggest a cooling from ~80 °C to approximately 30 °C. Assuming geothermal gradients between 20 and 30 °C/km, this would imply in a denudation of rock covers with thicknesses between 1.6 and 2.5 km.

The onset of this late Cretaceous to early Paleogene exhumation is recorded through most of the passive margin in southeast Brazil, particularly in its central portion, where it is associated with the uplift of the elevated coast-parallel ridges (Cogné et al., 2011, 2012; Hackspacher et al., 2004, 2007; Hiruma et al., 2010; Tello Saenz et al., 2003). It postdates the rifting of the South Atlantic opening by at least 40 Myr and, as such, cannot be assigned to the early development stages of the passive margin (Green et al. 2018). In fact, this event is most commonly associated with the intrusion of alkaline magmatism and/or pronounced tectonic activity in the Andean system (Cobbold et al., 2001; Cogné et al., 2011, 2012). The latter hypothesis is commonly

interpreted to have been controlled by the normal reactivation of Neoproterozoic shear zones during uplift. This, however, is not the case in the study area, which recorded no significant vertical displacement along the main inherited structural feature.

Timing of the final exhumation to near-surface conditions is not uniform in the Dom Feliciano Belt. Available AHe and apatite fission track data in the southern exposures of the orogen are predominantly coeval with the onset of the Paraná LIP or younger, indicating that most of the belt was already exposed to near-surface conditions prior to the South Atlantic rifting (Hueck et al., 2017; Oliveira et al., 2015). Hence, the distinct responses to exhumation stages along the passive margin are probably controlled by transverse structures with NW-SE orientation, associated with the early stages of continental break-up and rotation of the South American plate (Salomon et al., 2017; Szatmari & Milani, 2016). These structures are associated with the doming of the sediments of the Paraná Basin (Milani et al., 2007; Rostirolla et al., 2000) and with the formation of the main fracture zones in the South Atlantic (Stica et al., 2014; Torsvik et al., 2009). Karl et al. (2013), recognizing the effect of this segmentation in the thermochronological record of the passive margin, included the study area in one of these blocks, characterized by older ZHe and zircon fission track ages. The exhumation constrained in this study, in the order of 1.6–2.5 km, thus exemplifies the significance of the NW-SE structures in controlling the postrift development of the passive margin.

6.3. Comparing Zircon Radiation Damage Ages and the ZHe Ages

Most zircon radiation ages calculated in this study have a range that corresponds to the reasonable time interval expected from the geological context. Few crystals yielded outlying ages that are probably a reflection of the limitations of assuming that punctual Raman analyses are representative of the entire crystal. Unrealistic old ages, in part older than the crystallization age of the sampled rocks, were probably obtained from crystal zones with elevated U and Th concentration. The inverse can be assumed for exceedingly young ages, in particular those younger than the age of the onset of the Paraná LIP, which is the last important heating event in the study area. Future research exploring this method should use a statistical approach to Raman measurements in order to define values that are more representative of the entire crystal, so as to allow for more confident direct comparisons with the (U-Th)/He method.

Nonetheless, the new data set produces some important correlations between the two systems. The apparent ZHe ages have similar ranges that appear to be geologically consistent but lack a direct correlation. The radiation damage ages mirror the ZHe results in the sense that they present a wide range of ages, which is unexpected for samples that are interpreted to have experienced a similar thermal evolution. Both systems also produced ages that are mostly restricted between ~ 500 and 130 Ma. Therefore, it may be hypothesized that the radiation damage ages also represent a system that has been allowed to accumulate since ~500 Ma and was partially rest at ~130 Ma, due to the onset of the Paraná LIP.

A consequence of this observation is that the measured zircons must have been subjected to some degree of healing of its crystalline lattices and that this process took place under temperature conditions between ~180 and 220 °C, as constrained by the eU-based modeling of the ZHe ages. These temperature conditions are lower than expected, as the annealing of radiation damage in zircon is commonly interpreted to occur at temperatures similar to those of fission track annealing, which are usually estimated between 200 and 250 °C (Bernet, 2009; Yamada et al., 1995). However, single crystal He ages do not correlate with corresponding radiation damage ages, probably as an expression of the considerable imprecision of both methods, including the question of representability of the Raman spot analyses. As such, it is not possible to estimate the temperatures involved in the annealing of individual zircon crystals. Nonetheless, radiation damage ages in our study are consistently older than those obtained from the (U-Th)/He system, which probably has a systematic significance. This indicates that in our study area, the diffusion of He in zircon crystals was more effective than the annealing of radiation damage during the Cretaceous thermal overprint. Both processes are dependent not only of the temperature to which the systems were exposed to but also of the duration of the thermal event. As our results are interpreted to represent the impact of elevated heating during a short period, it would be interesting to investigate the relationship between both methods in areas which experienced long exposures to temperatures close to the ZHe PRZ.

A final interesting observation in our data set is the correlation between radiation damage ages and eU content (Figure 5). This is somewhat unexpected, as the ages are calculated from a calibration curve that already

expresses the effect of radioactive concentration in the crystals (Nasdala et al., 2001; Pidgeon, 2014). As such, this correlation may suggest that the annealing of radiation damage is susceptible to the degree of damage already experienced by the crystal, which would implicate that different healing mechanism are active for crystals with different damage densities. The younger radiation damage ages in crystals with more elevated eU contents, which are expected to have accumulated more damage, indicate they were more effectively annealed during the thermal overprint.

In summary, the results in this data set illustrate how the dynamics of radiation damage healing and its applicability for dating are still poorly understood (e.g., Pidgeon, 2014, and references therein). However, the degree of concordance with the ZHe system presented in our data set is promising and deserves to be further explored as a companion for more established thermochronologic methods. At the very least, Raman spectroscopy can be used to quickly estimate radiation damage and consequently select less disturbed crystals for (U-Th)/He dating, when the aim is to obtain more significant individual apparent ages.

7. Conclusion

New thermochronologic data reveal a well-constrained Phanerozoic thermal history for a segment of the South American passive margin, thanks to modeling contrasting patterns of eU versus He age for zircon and apatite. Widespread apparent ZHe ages span most of the Phanerozoic and are strongly eU dependent, indicating a partially reset system which has experienced relative low temperatures since at least the early Paleozoic. Exposition to surface conditions prior to the sedimentation of the intracratonic Paraná Basin is probable, but modeling of the ZHe data set indicate that this burial had relatively little impact on the basement. The most likely cause for its partial reset is the onset of the Paraná LIP in the Lower Cretaceous. After this event, the study area was probably covered by up to 2 km of basaltic floods, keeping the AHe system open until rapid postrift cooling between 75 and 55 Ma, as constrained by thermal modeling. Despite the presence of the Major Gercino Shear Zone, an important crustal discontinuity, the thermochronologic data set does not appear to have experienced differential exhumation, and whichever reactivations of the shear zone happened during the Phanerozoic were not enough to leave an imprint in the new data set. The thermal imprint revealed by the data set and attributed to the Paraná LIP is interesting, as the volcanic floods are not expected to have contributed with heat for enough time to affect the ZHe system of the strata below. We propose that the longer-lived elevated geothermal gradient suggested by our data set was caused by the intrusion of the Florianópolis Dyke Swarm, an important feeder system of the LIP that may be related to its central ridge. The successful modeling of the widespread ZHe data set into a coherent geological history evidences the risks of overinterpretation of apparent (U-Th)/He ages in a context where radiation damage accumulation may lead to variable closure temperatures. For this reason, it is important to develop companion systems that can act as independent validation. As shown in this work, the assessment of zircon radiation damage by Raman spectroscopy is a promising method that should be better developed.

Acknowledgments
Data for this paper are available in the supporting information S1. Mathias Hueck would like to thank the CNPq for a long-term PhD scholarship from the Sciences without Borders program. The authors would also like to thank editors John Geissman and Cornelia Speigel for the editorial handling and Raphaël Pik and an unknown reviewer for critical comments that helped improve the manuscript.

References

Almeida, F. F. M., Hasui, Y., de Brito Neves, B. B., & Fuck, R. A. (1981). Brazilian structural provinces; an introduction. *Earth-Science Reviews*, *17*(1-2), 1–29. https://doi.org/10.1016/0012-8252(81)90003-9

Assine, M. L., Soares, P. C., & Milani, E. J. (1994). Sequências tectono-sedimentares mesopaleozóicas da Bacia do Paraná, Sul do Brasil. *Revista Brasileira de Geociencias*, *24*(2), 77–89. https://doi.org/10.25249/0375-7536.19947789

Ault, A. K., & Flowers, R. M. (2012). Is apatite U–Th zonation information necessary for accurate interpretation of apatite (U–Th)/He thermochronometry data? *Geochimica et Cosmochimica Acta*, *79*, 60–78. https://doi.org/10.1016/j.gca.2011.11.037

Ault, A. K., Flowers, R. M., & Bowring, S. A. (2009). Phanerozoic burial and unroofing history of the western Slave craton and Wopmay orogen from apatite (U–Th)/He thermochronometry. *Earth and Planetary Science Letters*, *284*(1-2), 1–11. https://doi.org/10.1016/j.epsl.2009.02.035

Basei, M. A. S., Campos Neto, M. C., Castro, N. A., Nutman, A. P., Wemmer, K., Yamamoto, M. T., et al. (2011). Tectonic evolution of the Brusque group, Dom Feliciano belt, Santa Catarina, southern Brazil. *Journal of South American Earth Sciences*, *32*(4), 324–350. https://doi.org/10.1016/j.jsames.2011.03.016

Basei, M.A.S., Campos Neto, M.C., Castro, N.A., Santos, P.R., Siga Jr., O., Passarelli, C.R. (2006). Mapa Geológico 1:100,000 das Folhas Brusque e Vidal Ramos, SC, Convênio USP-CPRM. Paper presented at the 42nd Congresso Brasileiro de Geologia, Aracaju, Brazil.

Basei, M. A. S., Campos Neto, M. C., Lopes, A. P., Nutman, A. P., Liu, D., & Sato, K. (2013). Polycyclic evolution of Camboriú Complex migmatites, Santa Catarina, Southern Brazil: Integrated Hf isotopic and U-Pb age zircon evidence of episodic reworking of a Mesoarchean juvenile crust. *Brazilian Journal of Geology*, *43*(3), 427–443. https://doi.org/10.5327/Z2317-48892013000300002

Basei, M. A. S., Drukas, C. O., Nutman, A., Wemmer, P. K., Dunyi, L., Santos, P. R., et al. (2011). The Itajaí foreland basin: A tectono-sedimentary record of the Ediacaran period, southern Brazil. *International Journal of Earth Sciences*, *100*(2-3), 543–569. https://doi.org/10.1007/s00531-010-0604-4

Basei, M. A. S., Nutman, A., Siga, O. Jr., Passarelli, C. R., & Drukas, C. O. (2009). The evolution and tectonic setting of the Luis Alves Microplate of Southeastern Brazil: An exotic terrane during the assembly of Western Gondwana. In C. Gaucher, A. N. Sial, G. P. Halverson, & H. E. Frimmel (Eds.), *Neoproterozoic-Cambrian tectonics, global change and evolution: A focus on southwestern Gondwana, Developments in Precambrian Geology*, (Vol. 16, pp. 273–291). Elsevier. https://doi.org/10.1016/S0166-2635(09)01620-X

Basei, M. A. S., Siga, O. Jr., Masquelin, H., Harara, O. M., Reis Neto, J. M., & Preciozzi, F. (2000). The Dom Feliciano Belt of Brazil and Uruguay and its foreland domain the Rio de la Plata craton: Framework, tectonic evolution and correlation with similar provinces of southwestern Africa. In U. G. Cordani, E. J. Milani, A. Thomaz Filho, & D. A. Campos (Eds.), *Tectonic Evolution of South America*, (pp. 311–334). Rio de Janeiro: IGC 31.

Bernet, M. (2009). A field-based estimate of the zircon fission-track closure temperature. *Chemical Geology*, *259*(3–4), 181–189. https://doi.org/10.1016/j.chemgeo.2008.10.043

Bitencourt, M. F., & Kruhl, J. H. (2000). Crustal-scale shearing, magmatism and the development of deformation structures: An example from Santa Catarina (Southern Brazil). *Zeitschrift für Angewandte Geologie*, *SH1/2000*, 229–236.

Bitencourt, M. F., & Nardi, L. V. S. (2000). Tectonic setting and sources of magmatism related to the Southern Brazilian shear Belt. *Revista Brasileira de Geociencias*, *30*(1), 186–189. https://doi.org/10.25249/0375-7536.2000301186189

Brito Neves, B. B., & Fuck, R. A. (2014). The basement of the South American platform: Half Laurentian (N-NW) + half Gondwanan (E-SE) domains. *Precambrian Research*, *244*, 75–86. https://doi.org/10.1016/j.precamres.2013.09.020

Chemale, F., Mallmann, G., Bitencourt, M. F., & Kawashita, K. (2012). Time constraints on magmatism along the Major Gercino Shear Zone, southern Brazil: Implications for West Gondwana reconstruction. *Gondwana Research*, *22*(1), 184–199. https://doi.org/10.1016/j.gr.2011.08.018

Cobbold, P. R., Meisling, K. E., & Mount, V. S. (2001). Reactivation of an obliquely rifted margin, Campos and Santos Basins, Southeastern Brazil. *AAPG Bulletin*, *85*, 1925–1944.

Cogné, N., Gallagher, K., & Cobbold, P. R. (2011). Post-rift reactivation of the onshore margin of Southeast Brazil: Evidence from apatite (U–Th)/He and fission-track data. *Earth and Planetary Science Letters*, *309*(1-2), 118–130. https://doi.org/10.1016/j.epsl.2011.06.025

Cogné, N., Gallagher, K., Cobbold, P. R., Riccomini, C., & Gautheron, C. (2012). Post-breakup tectonics in Southeast Brazil from thermochronological data and combined inverse-forward thermal history modelling. *Solid Earth*, *117*(B11). https://doi.org/10.1029/2012JB009340

Contreras, J., Zühlke, R., Bowman, S., & Bechstädt, T. (2010). Seismic stratigraphy and subsidence analysis of the southern Brazilian margin (Campos, Santos and Pelotas basins). *Marine and Petroleum Geology*, *27*(9), 1952–1980. https://doi.org/10.1016/j.marpetgeo.2010.06.007

Danišík, M., McInnes, B. I., Kirkland, C. L., McDonald, B. J., Evans, N. J., & Becker, T. (2017). Seeing is believing: Visualization of He distribution in zircon and implications for thermal history reconstruction on single crystals. *Science Advances*, *3*(2), e1601121. https://doi.org/10.1126/sciadv.1601121

Dunkl, I., Mikes, T., Simon, K., & von Eynatten, H. (2008). Brief introduction to the Windows program Pepita: Data visualization, and reduction, outlier rejection, calculation of trace element ratios and concentrations from LAICPMS data. *Mineralogical Association of Canada, Short Course*, *40*, 334–340.

Ernesto, M., Raposo, M. I. B., Marques, L. S., Renne, P. R., Diogo, L. A., & de Min, A. (1999). Paleomagnetism, geochemistry and $^{40}Ar/^{39}Ar$ dating of the North-eastern Paraná Magmatic Province: Tectonic implications. *Journal of Geodynamics*, *28*(4–5), 321–340. https://doi.org/10.1016/S0264-3707(99)00013-7

Farley, K. A., Wolf, R. A., & Silver, L. T. (1996). The effects of long alpha-stopping distances on (U-Th)/He ages. *Geochimica et Cosmochimica Acta*, *60*(21), 4223–4229. https://doi.org/10.1016/S0016-7037(96)00193-7

Florisbal, L. M., Heaman, L. M., de Assis Janasi, V., & Bitencourt, M. F. (2014). Tectonic significance of the Florianópolis Dyke Swarm, Paraná–Etendeka Magmatic Province: A reappraisal based on precise U–Pb dating. *Journal of Volcanology and Geothermal Research*, *289*, 140–150. https://doi.org/10.1016/j.jvolgeores.2014.11.007

Florisbal, L. M. F., Janasi, V. A., Bitencourt, M. F., & Heaman, L. M. (2012). Space-time relation of post-collisional granitic magmatism in Santa Catarina, southern Brazil: U-Pb LAMC-ICP-MS zircon geochronology of coeval mafic-felsic magmatism related to the Major Gercino Shear Zone. *Precambrian Research*, *216-219*, 132–151. https://doi.org/10.1016/j.precamres.2012.06.015

Flowers, R., Ketcham, R. A., Shuster, D. L., & Farley, K. A. (2009). Apatite (U–Th)/He thermochronometry using a radiation damage accumulation and annealing model. *Geochimica et Cosmochimica Acta*, *73*(8), 2347–2365. https://doi.org/10.1016/j.gca.2009.01.015

Flowers, R. M., & Kelley, S. A. (2011). Interpreting data dispersion and inverted dates in apatite (U–Th)/He and fission-track datasets: An example from the U.S. mid-continent. *Geochimica et Cosmochimica Acta*, *75*(18), 5169–5186. https://doi.org/10.1016/j.gca.2011.06.016

Foster, D. A., Goscombe, B. D., & Gray, D. R. (2009). Rapid exhumation of deep crust in an obliquely convergent orogeny: The Kaoko Belt of the Damara Orogen. *Tectonics*, *28*, TC4002. https://doi.org/10.1029/2008TC002317

Franco-Magalhaes, A. O. B., Cuglieri, M. A. A., Hackspacher, P. C., & Saad, A. R. (2014). Long-term landscape evolution and post-rift reactivation in the southeastern Brazilian passive continental margin: Taubaté basin. *International Journal of Earth Sciences*, *103*(2), 441–453. https://doi.org/10.1007/s00531-013-0967-4

Franco-Magalhães, A. O. B., Hackspacher, P. C., Glasmacher, U. A., & Saad, A. R. (2010). Rift to post-rift evolution of a "passive" continental margin: The Ponta Grossa Arch, SE Brazil. *International Journal of Earth Sciences*, *99*(7), 1599–1613. https://doi.org/10.1007/s00531-010-0556-8

Gautheron, C., Barbarand, J., Ketcham, R. A., Tassan-Got, L., van der Beek, P., Pagel, M., et al. (2013). Chemical influence on α-recoil damage annealing in apatite: Implications for (U–Th)/He dating. *Chemical Geology*, *351*, 257–267. https://doi.org/10.1016/j.chemgeo.2013.05.027

Goscombe, B., Gray, D., Armstrong, R., Foster, D. A., & Vogl, J. (2005). Event geochronology of the Pan-African Kaoko Belt, Namibia. *Precambrian Research*, *140*, 103.e1–103.e41.

Gray, D. R., Foster, D. A., Goscombe, B., Passchier, C. W., & Trouw, R. A. J. (2006). $^{40}Ar/^{39}Ar$ thermochronology of the Pan-African Damara Orogen, Namibia with implications for tectonothermal and geodynamic evolution. *Precambrian Research*, *150*(1-2), 49–72. https://doi.org/10.1016/j.precamres.2006.07.003

Green, P. F., Japsen, P., Chalmers, J. A., Bonow, J. M., & Duddy, I. R. (2018). Post-breakup burial and exhumation of passive continental margins: Seven propositions to inform geodynamic models. *Gondwana Research*, *53*, 58–81. https://doi.org/10.1016/j.gr.2017.03.007

Guadagnin, F., Chemale, F. Jr., Dussin, I. A., Jelinek, A. R., Santos, M. N., Borba, M. L., et al. (2010). Depositional age and provenance of the Itajaí Basin, Santa Catarina State, Brazil: Implications for SW Gondwana correlation. *Precambrian Research*, *180*(3-4), 156–182. https://doi.org/10.1016/j.precamres.2010.04.002

Guenthner, W. R., Reiners, P. W., DeCelles, P. G., & Kendall, J. (2015). Sevier belt exhumation in central Utah constrained from complex zircon (U-Th)/He data sets: Radiation damage and He inheritance effects on partially reset detrital zircons. *Geological Society of America Bulletin*, *127*. https://doi.org/10.1130/B31032.1

Guenthner, W. R., Reiners, P. W., Drake, H., & Tillberg, M. (2017). Zircon, titanite, and apatite (U-Th)/He ages and age-eU correlations from the Fennoscandian Shield, southern Sweden. *Tectonics*, *36*, 1254–1274. https://doi.org/10.1002/2017TC004525

Guenthner, W. R., Reiners, P. W., Ketcham, R. A., Nasdala, L., & Giester, G. (2013). Helium diffusion in natural zircon: Radiation damage, anisotropy, and the interpretation of zircon (U-Th)/He thermochronology. *American Journal of Science*, *313*(3), 145–198. https://doi.org/10.2475/03.2013.01

Hackspacher, P. C., Godoy, D. F., Ribeiro, L. F. B., Neto, J. C. H., & Franco, A. O. B. (2007). Modelagem térmica e geomorfologia da borda sul do Cráton do São Francisco: termocronologia por traços de fissão em apatita. *Revista Brasileira de Geociencias*, *37*(S4), 76–86. https://doi.org/10.25249/0375-7536.200737S47686

Hackspacher, P. C., Ribeiro, L. F. B., Ribeiro, M. C. S., Fetter, A. H., Hadler Neto, J. C., Tello Saenz, C. A., & et al. (2004). Consolidation and break-up of the South American platform in southeastern Brazil: Tectonothermal and denudation histories. *Gondwana Research*, *1*, 91–101.

Heilbron, M., Valeriano, C. M., Tassinari, C. C. G., Almeida, J., Tupinambá, M., Siga, O., & Trouw, R. (2008). Correlation of Neoproterozoic terranes between the Ribeira Belt, SE Brazil and its African counterpart: Comparative tectonic evolution and open questions. *Geological Society, London, Special Publications*, *294*(1), 211–237. https://doi.org/10.1144/SP294.12

Hiruma, S. T., Riccomini, C., Modenesi-Gauttieri, M. C., Hackspacher, P. C., Hadler Neto, J. C., & Franco-Magalhães, A. O. B. (2010). Denudation history of the Bocaina Plateau, Serra do Mar, Southeastern Brazil: Relationships to Gondwana breakup and passive margin development. *Gondwana Research*, *18*(4), 674–687. https://doi.org/10.1016/j.gr.2010.03.001

Holz, M., França, A. B., Souza, P. A., Iannuzzi, R., & Rohn, R. (2010). A stratigraphic chart of the Late Carboniferous/Permian succession of the eastern border of the Paraná Basin, Brazil, South America. *Journal of South American Earth Sciences*, *29*(2), 381–399. https://doi.org/10.1016/j.jsames.2009.04.004

Hueck, M., Basei, M. A. S., & de Castro, N. A. (2016). Origin and evolution of the granitic intrusions in the Brusque Group of the Dom Feliciano Belt, south Brazil: Petrostructural analysis and whole-rock/isotope geochemistry. *Journal of South American Earth Sciences*, *69*, 131–151. https://doi.org/10.1016/j.jsames.2016.04.004

Hueck, M., Oriolo, S., Dunkl, I., Wemmer, K., Oyhantçabal, P., Schanofski, M., et al. (2017). Phanerozoic low-temperature evolution of the Uruguayan Shield along the South American passive margin. *Journal of the Geological Society of London*, *174*(4), 609–626. https://doi.org/10.1144/jgs2016-101

Hueck, M., Oyhantçabal, P., Philipp, R.P., Basei, M.A.S., Siegesmund, S. (2018). The Dom Feliciano Belt in Southern Brazil and Uruguay. In: Siegesmund, S., Oyhantçabal, P., Basei, M.A.S., Oriolo, S. (Eds.), *Geology of Southwest Gondwana*, Regional geology reviews (pp. 267–302). Springer, Heidelberg. https://doi.org/10.1007/978-3-319-68920-3_11

Hurter, S. J., & Pollack, H. N. (1994). Effect of the Cretaceous Serra Geral igneous event on the temperatures and heat flow of the Paraná Basin, southern Brazil. *Basin Research*, *6*(4), 239–244. https://doi.org/10.1111/j.1365-2117.1994.tb00087.x

Irmer, G. (1985). Zum Einfluß der Apparatefunktion auf die Bestimmung von Streuquerschnitten und Lebensdauern aus optischen Phononenspektren. *Experimentelle Technik der Physik*, *33*(6), 501–506.

Janasi, V. A., Freitas, V. A., & Heaman, L. H. (2011). The onset of flood basalt volcanism, Northern Paraná Basin, Brazil: A precise U–Pb baddeleyite/zircon age for a Chapecó-type dacite. *Earth and Planetary Science Letters*, *302*(1-2), 147–153. https://doi.org/10.1016/j.epsl.2010.12.005

Jelinek, A. R., Chemale, F. C. Jr., van der Beek, P. A., Guadagnin, F., Cupertino, J. A., & Viana, A. (2014). Denudation history and landscape evolution of the northern east-Brazilian continental margin from apatite fission-track thermochronology. *Journal of South American Earth Sciences*, *54*, 158–181. https://doi.org/10.1016/j.jsames.2014.06.001

Johnson, J. E., Flowers, R. M., Baird, G. B., & Mahan, K. H. (2017). "Inverted" zircon and apatite (U–Th)/He dates from the Front Range, Colorado: High-damage zircon as a low-temperature (<50°C) thermochronometer. *Earth and Planetary Sciences*, *466*, 80–90. https://doi.org/10.1016/j.epsl.2017.03.002

Karl, M., Glasmacher, U. A., Kollenz, S., Franco-Magalhaes, A. O. B., Stockli, D. F., & Hackspacher, P. C. (2013). Evolution of the South Atlantic passive continental margin in southern Brazil derived from zircon and apatite (U–Th–Sm)/He and fission-track data. *Tectonophysics*, *604*, 224–244. https://doi.org/10.1016/j.tecto.2013.06.017

Ketcham, R. A. (2005). Forward and inverse modeling of low-temperature thermochronometry data. *Reviews in Mineralogy and Geochemistry*, *58*(1), 275–314. https://doi.org/10.2138/rmg.2005.58.11

Kollenz, S., Glasmacher, U. A., Rossello, E. A., Stockli, D. F., Schad, S., & Pereyra, R. E. (2016). Thermochronological constraints on the Cambrian to recent geological evolution of the Argentina passive continental margin. *Tectonophysics*, *716*, 182–203.

Lünsdorf, N. K., & Lünsdorf, J. O. (2016). Evaluating Raman spectra of carbonaceous matter by automated, iterative curve-fitting. *International Journal of Coal Geology*, *160-161*, 51–62. https://doi.org/10.1016/j.coal.2016.04.008

Milani, E. J., Melo, J. H. G., Souza, P. A., Fernandes, L. A., & França, A. B. (2007). Bacia do Paraná. In E. J. Milani, H. D. Rangel, G. V. Bueno, J. M. Stica, W. R. Winter, J. M. Caixeta, & O. C. Pessoa Neto (Eds.), *Bacias Sedimentares Brasileiras—Cartas Estratigráficas*, (Vol. 15, pp. 265–287). Rio de Janeiro, Brazil: Boletim de Geociências da Petrobras.

Moulin, M., Aslanian, D., & Unternehr, P. (2010). A new starting point for the South and Equatorial Atlantic Ocean. *Earth-Science Reviews*, *98*(1–2), 1–37. https://doi.org/10.1016/j.earscirev.2009.08.001

Murray, K. E., Reiners, P. W., & Thomson, S. N. (2016). Rapid Pliocene–Pleistocene erosion of the central Colorado Plateau documented by apatite thermochronology from the Henry Mountains. *Geology*, *44*(6), 483–486. https://doi.org/10.1130/G37733.1

Nasdala, L., Wenzel, M., Vavra, G., Irmer, G., Wenzel, T., & Kober, B. (2001). Metamictisation of natural zircon: Accumulation versus thermal annealing of radioactivity-induced damage. *Contributions to Mineralogy and Petrology*, *141*(2), 125–144. https://doi.org/10.1007/s004100000235

Oliveira, C. H. E., Jelinek, A. R., Chemale, F. Jr., & Bernet, M. (2015). Evidence of post-Gondwana breakup in Southern Brazilian Shield: Insights from apatite and zircon fission track thermochronology. *Tectonophysics*, *666*, 173–187.

Oriolo, S., Hueck, M., Oyhantçabal, P., Goscombe, B., Wemmer, K., & Siegesmund, S. (2018). Shear zones in Brasiliano-Pan-African belts and their role in the amalgamation and break-up of southwest Gondwana. In S. Siegesmund, P. Oyhantçabal, M. A. S. Basei, & S. Oriolo (Eds.), *Geology of Southwest Gondwana, Regional Geology Reviews*, (pp. 593–613). Heidelberg: Springer. https://doi.org/10.1007/978-3-319-68920-3_22

Oriolo, S., Oyhantçabal, P., Wemmer, K., Heidelbach, F., Pfänder, J., Basei, M. A. S., et al. (2016). Shear zone evolution and timing of deformation in the Neoproterozoic transpressional Dom Feliciano Belt, Uruguay. *Journal of Structural Geology*, *92*, 59–78. https://doi.org/10.1016/j.jsg.2016.09.010

Orme, D. A., Guenthner, W. R., Laskowski, A. K., & Reiners, P. W. (2016). Long-term tectonothermal history of Laramide basement from zircon–He age-eU correlations. *Earth and Planetary Science Letters*, *453*, 119–130. https://doi.org/10.1016/j.epsl.2016.07.046

Oyhantçabal, P., Siegesmund, S., Wemmer, K., Presnyakov, S., & Layer, P. (2009). Geochronological constraints on the evolution of the southern Dom Feliciano Belt (Uruguay). *Journal of the Geological Society of London*, *166*(6), 1075–1084. https://doi.org/10.1144/0016-76492008-122

Palenik, C. S., Nasdala, L., & Ewing, R. C. (2003). Radiation damage in zircon. *American Mineralogist*, *88*(5–6), 770–781. https://doi.org/10.2138/am-2003-5-606

Passarelli, C. R., Basei, M. A. S., Siga, O. Jr., & Harara, M. M. (2018). The Luis Alves and Curitiba terranes: Continental fragments in the Adamastor Ocean. In S. Siegesmund, P. Oyhantçabal, M. A. S. Basei, & S. Oriolo (Eds.), *Geology of Southwest Gondwana, Regional Geology Reviews*, (pp. 161–188). Heidelberg: Springer.

Passarelli, C. R., Basei, M. A. S., SigaMc Reath, I. Jr., & Campos Neto, M. C. (2010). Deformation and geochronology of syntectonic granitoids emplaced in the major Gercino Shear zone, southeastern south America. *Gondwana Research*, *17*(4), 688–703. https://doi.org/10.1016/j.gr.2009.09.013

Passarelli, C. R., Basei, M. A. S., Wemmer, K., Siga, O. Jr., & Oyhantçabal, P. (2011). Major shear zones of southern Brazil and Uruguay: Escape tectonics in the eastern border of Rio de La Plata and Paranapanema cratons during the Western Gondwana amalgamation. *International Journal of Earth Sciences*, *100*(2-3), 391–414. https://doi.org/10.1007/s00531-010-0594-2

Philipp, R. P., Mallmann, G., Bitencourt, M. F., Souza, E. R., Souza, M. M. A., Liz, J. D., et al. (2004). Caracterização litológica e evolução metamórfica da porção leste do Complexo Metamórfico Brusque, Santa Catarina. *Revista Brasileira de Geociencias*, *34*(1), 21–34. https://doi.org/10.25249/0375-7536.20043412134

Philipp, R. P., Pimentel, M. M., & Chemale, F. Jr. (2016). Tectonic evolution of the Dom Feliciano Belt in southern Brazil: Geological relationships and U-Pb geochronology. *Brazilian Journal of Geology*, *46*(suppl 1), 83–104. https://doi.org/10.1590/2317-4889201620150016

Pidgeon, R. T. (2014). Zircon radiation damage ages. *Chemical Geology*, *367*, 13–22. https://doi.org/10.1016/j.chemgeo.2013.12.010

Powell, J., Schneider, D., Stockli, D., & Fallas, K. (2016). Zircon (U-Th)/he thermochronology of Neoproterozoic strata from the Mackenzie Mountains, Canada: Implications for the Phanerozoic exhumation and deformation history of the northern Canadian Cordillera. *Tectonics*, *35*, 663–689. https://doi.org/10.1002/2015TC003989

Renne, P. R., Ernesto, M., Pacca, I. G., Coe, R. S., Glen, J. M., Prévot, M., & Perrin, M. (1992). The age of ParanJ flood volcanism, rifting of Gondwanaland, and the Jurassic-Cretaceous boundary. *Science*, *258*(5084), 975–979. https://doi.org/10.1126/science.258.5084.975

Ribeiro, L. F. B., Hackspacher, P. C., Ribeiro, M. C. S., Hadler Neto, J. C., Tello, S. C. A., Iunes, P. J., et al. (2005). Thermotectonic and fault dynamic analysis of Precambrian basement and tectonic constraints with the Parana basin. *Radiation Measurements*, *39*(6), 669–673. https://doi.org/10.1016/j.radmeas.2004.09.007

Riccomini, C. (1997). Arcabouço estrutural e aspectos do tectonismo gerador e deformador da Bacia Bauru no Estado de São Paulo. *Revista Brasileira de Geociencias*, *27*(2), 153–162. https://doi.org/10.25249/0375-7536.1997153162

Rocha Campos, A. C., Basei, M. A. S., Nutman, A. P., dos Santos, P. R. (2007). SHRIMP U-Pb zircon geochronological calibration of the late Paleozoic supersequence, Paraná Basin, Brazil. Paper presented at the 4th Simpósio Sobre Cronoestratigrafia da Bacia do Paraná, Armação de Búzios, Brazil.

Rostirolla, S. P., Alckmin, F. F., & Soares, P. C. (1992). O Grupo Itajaí, Estado de Santa Catarina, Brasil, exemplo de sedimentação em uma bacia flexural de antepaís. *Boletim de Geociências da Petrobrás*, *6*(3/4), 109–122.

Rostirolla, S. P., Assine, M. L., Fernandes, L. A., & Artur, P. C. (2000). Reativação de paleolineamentos durante a evolução da Bacia do Paraná—O exemplo do alto estrutural de Quatiguá. *Revista Brasileira de Geociencias*, *30*(4), 639–648. https://doi.org/10.25249/0375-7536.2000304639648

Salomon, E., Passchier, C., & Koehn, D. (2017). Asymmetric continental deformation during South Atlantic rifting along southern Brazil and Namibia. *Gondwana Research*, *51*, 170–176. https://doi.org/10.1016/j.gr.2017.08.001

Schultz, M. H., Hodges, K. V., Ehlers, T. A., van Soest, M., & Wartho, J. A. (2017). Thermochronologic constraints on the slip history of the South Tibetan detachment system in the Everest region, southern Tibet. *Earth and Planetary Science Letters*, *459*, 105–117. https://doi.org/10.1016/j.epsl.2016.11.022

Silva, L. C., Armstrong, R., Pimentel, M. M., Scandolara, J., Ramgrab, G., Wildner, W., et al. (2002). Reavaliação da evolução geológica em terrenos pré-cambrianos brasileiros com base em novos dados U-Pb SHRIMP, Parte III: Províncias Borborema, Mantiqueira Meridional e Rio Negro-Juruena. *Revista Brasileira de Geociencias*, *32*(4), 529–544. https://doi.org/10.25249/0375-7536.2002324529544

Silva, Z. C. C., & Cornford, C. (1985). The kerogen type, depositional environment and maturity, of the Irati shale, Upper Permian of Paraná Basin, southern Brazil. *Organic Geochemistry*, *8*(6), 399–411. https://doi.org/10.1016/0146-6380(85)90018-X

Spiegel, C., Kohn, B., Belton, D., Berner, Z., & Gleadow, A. (2009). Apatite (U–Th–Sm)/He thermochronology of rapidly cooled samples: The effect of He implantation. *Earth and Planetary Science Letters*, *285*(1-2), 105–114. https://doi.org/10.1016/j.epsl.2009.05.045

Stica, J. M., Zalán, P. V., & Ferrari, A. L. (2014). The evolution of rifting on the volcanic margin of the Pelotas Basin and the contextualization of the Paraná-Etendeka LIP in the separation of Gondwana in the South Atlantic. *Marine and Petroleum Geology*, *50*, 1–21. https://doi.org/10.1016/j.marpetgeo.2013.10.015

Sueoka, S., Kohn, B. P., Tagami, T., Tsutsumi, H., Hasebe, N., Tamura, A., & Arai, S. (2012). Denudation history of the Kiso range, Central Japan, and its tectonic implications: Constraints from low-temperature thermochronology. *Island Arc*, *21*(1), 32–52. https://doi.org/10.1111/j.1440-1738.2011.00789.x

Szatmari, P., & Milani, E. J. (2016). Tectonic control of the oil-rich large igneous-carbonate-salt province of the South Atlantic rift. *Marine and Petroleum Geology*, *77*, 567–596. https://doi.org/10.1016/j.marpetgeo.2016.06.004

Tagami, T. (2012). Thermochronological investigation of fault zones. *Tectonophysics*, *538-540*, 67–85. https://doi.org/10.1016/j.tecto.2012.01.032

Tello Saenz, C. A., Hackspacher, P. C., Hadler, N. J. C., Iunes, P. J., Guedes, S., Paulo, S. R., & Ribeiro, L. F. B. (2003). Recognition of cretaceous, Paleocene and Neogene tectonic reactivation, through apatite fission-track analysis in Precambrian areas of the Southeast Brazil: Association with the South Atlantic Ocean Opening. *Journal of South American Earth Sciences*, *15*, 137–142.

Thiede, D. S., & Vasconcelos, P. M. (2010). Parana flood basalts: Rapid extrusion hypothesis confirmed by new $^{40}Ar/^{39}Ar$ results. *Geology*, *38*(8), 747–750. https://doi.org/10.1130/G30919.1

Torsvik, T. H., Rousse, S., Labails, C., & Smethurst, M. A. (2009). A new scheme for the opening of the South Atlantic Ocean and the dissection of an Aptian salt basin. *Geophysical Journal International*, *177*(3), 1315–1333. https://doi.org/10.1111/j.1365-246X.2009.04137.x

Yamada, R., Tagami, T., Nishimura, S., & Ito, H. (1995). Annealing kinetics of fission tracks in zircon: An experimental study. *Chemical Geology*, *122*(1–4), 249–258. https://doi.org/10.1016/0009-2541(95)00006-8

Zalán, P. V., Wolff, S., Astolfi, M. A. M., Vieira, I. S., Conceição, J. C. J., Appi, V. T., et al. (1990). The Paraná Basin, Brazil. In M. W. Leighton, D. R. Kolata, D. F. Oltz, & J. J. Eidel (Eds.), *Interior cratonic basins*, Memoir of the American Association of Petroleum Geologists, (Vol. *51*, pp. 681–708).

Zerfass, H., Chemale, F. Jr., Schultz, C. L., & Lavina, E. (2004). Tectonics and sedimentation in southern South America during Triassic. *Sedimentary Geology*, *166*(3-4), 265–292. https://doi.org/10.1016/j.sedgeo.2003.12.008